INSTITUTE OF PHYSICS PUBLISHING JOURNAL OF PHYSICS: CONDENSED MATTER

J. Phys.: Condens. Matter **16** (2004) S2953–S2966 PII: S0953-8984(04)80321-7

Molecule scattering from insulator and metal surfaces

Iryna Moroz[1], **Hailemariam Ambaye and J R Manson**

Department of Physics and Astronomy, Clemson University, Clemson, SC 29634, USA

Received 4 May 2004
Published 9 July 2004
Online at stacks.iop.org/JPhysCM/16/S2953
doi:10.1088/0953-8984/16/29/010

Abstract

Calculations are carried out and compared with data for the scattering of CH_4 molecules from a LiF(001) surface and for O_2 scattering from Al(111). The theory is a mixed classical-quantum formalism that includes energy and momentum transfers between the surface and projectile for translational and rotational motions as well as internal mode excitation of the projectile molecule. The translational and rotational degrees of freedom couple most strongly to multiphonon excitations of the surface and are treated with classical dynamics. Internal vibrational excitations of the molecules are treated with a semiclassical formalism with extension to arbitrary numbers of modes and arbitrary quantum numbers. Calculations show good agreement for the dependence on incident translational energy, incident beam angle and surface temperature when compared with data for energy-resolved intensity spectra and angular distributions.

1. Introduction

The scattering of small molecules by surfaces is a widely investigated area of research because it can give information on the molecule–surface interaction potential and provide insights into trapping, adsorption and eventually surface chemical reactions [1–31]. To gain a better understanding of the fundamental physical processes involved in the surface interaction, it is clear that one must control the initial state of the incident molecule through the use of molecular beams with well-defined energies and angles [32–34], and also measure the states of the final scattered products as well as any products left on the surface [1, 15]. In many such studies using well-defined incident beams it is found that a large and readily measurable fraction of the incident beam is scattered back away from the surface, possibly after having been temporarily trapped in a physisorption potential well [16, 32].

The purpose of this paper is to examine two of these recent experimental studies, the scattering of O_2 by Al(111) [35] and the scattering of CH_4 by LiF(001) [15], and to analyse this data using a mixed quantum-classical theory that has been developed for the scattering

[1] Permanent address: Institute of Applied Mathematics and Fundamental Science, National University, 'Lvivska Polytechnika', Lviv 79013, Ukraine.

of molecules from surfaces [36, 37]. This theory uses classical dynamics to describe the translational and rotational motion and semiclassical quantum mechanics to describe the internal molecular vibrational modes. It is shown that both angular distributions and energy-resolved spectra can be quantitatively explained by this theory. In addition to examining the experimentally measured spectra, calculations are presented predicting the rotational and internal mode excitation of the scattered molecules.

The O_2/Al(111) system was investigated using a scattering experiment because of an intriguing complementary experiment by Zoric *et al* that showed enhanced sticking of the oxygen molecules at hyperthermal incident energies, but only for incident angles in the neighbourhood of $\theta_i = 20^\circ$ [38]. They measured oxygen sticking coefficients to be less than 1% for incident energies less than 100 meV, rising to nearly unity for incident energies of around 1 eV. The anomalous enhanced sticking near $\theta_i = 20^\circ$ was measured for energies over 100 meV. The scattering experiment measured a corroborating decreased total scattering intensity at the same angles and similar incident energies at which the increased sticking was observed, and it has been suggested that this observation is due to a steering mechanism into a shallow molecular adsorption well localized on the surface unit cell [39]. Additional measurements were made of the scattered angular distributions as functions of incident angle and surface temperature at somewhat lower energies where the total reflectivity was measured to be over 90%, and it is these latter measurements that are examined here.

High precision molecular beam experiments have demonstrated that scattering of CH_4 can be measured from clean, controlled surfaces of the relatively non-reactive insulator LiF(001) [15] as well as from certain metals [40, 41]. Contamination of the surfaces due to dissociative reactions does build up but only over time periods of hundreds of seconds. Thus, the initial scattering is from clean surfaces and its study should be useful in clarifying the interaction dynamics of CH_4. The scattering data generated by the experiments of [15] was taken in the plane of scattering with the incident beam and detector separated by a fixed angle of 90°. The measurements consist of two types, total scattered intensities as a function of incident beam angle (angular distributions), and time-of-flight (TOF) energy-resolved spectra at fixed incident angle. Because this apparatus is constrained by a fixed angle of 90° between the incident beam and detector directions the angular distributions are not of the usual type in which the scattered intensity at all final angles is measured for a single fixed incident angle. Instead, the intensity at each final angle corresponds to a specific incident angle according to $\theta_f = 90^\circ - \theta_i$.

For both of these systems the primary channels of energy exchange are expected to be conversion of the incident translational energy into phonon excitation, rotational excitation of the molecule and excitation of internal vibrational modes of the molecule. These data were originally analysed in terms of two well-known theoretical models, the hard cubes model [42] and the washboard model [43], and in many cases good qualitative explanations of the results were obtained. Here, it is shown that both angular distributions and energy-resolved spectra can be quantitatively explained by the present mixed quantum-classical theory.

This paper is organized as follows: the next section gives a description of the theory used to analyse the experimental data, section 3 gives a discussion of the comparisons of calculations with measurements as well as calculated results for the probabilities of rotational and internal vibrational mode excitation, and some conclusions are drawn in section 4.

2. Theory

The interaction between a molecular projectile and the surface is described by a many-body Hamiltonian of the form $H = H^p + H^c + V$, where H^p is the Hamiltonian of the free projectile

including all internal degrees of freedom, H^{c} is the Hamiltonian of the unperturbed surface, and V is the interaction coupling the projectile and surface. The state-to-state transition rate for an incident molecular projectile with well defined initial translational momentum $\mathbf{p}_{\mathrm{i}}$, angular momentum $\mathbf{l}_{\mathrm{i}}$, and excitation quantum number $\alpha_{j\mathrm{i}}$ for the jth internal mode, which makes a transition to a final state denoted by $\mathbf{p}_{\mathrm{f}}$, $\mathbf{l}_{\mathrm{f}}$, and $\alpha_{l\mathrm{f}}$ is given by the generalized Fermi golden rule

$$w(\mathbf{p}_{\mathrm{f}}, \mathbf{l}_{\mathrm{f}}, \alpha_{l\mathrm{f}}; \mathbf{p}_{\mathrm{i}}, \mathbf{l}_{\mathrm{i}}, \alpha_{j\mathrm{i}}) = \left\langle\!\!\left\langle \frac{2\pi}{\hbar} \sum_{\{n_{\mathrm{f}}\}} |\mathcal{T}_{\mathrm{fi}}|^2 \, \delta(\mathcal{E}_{\mathrm{f}} - \mathcal{E}_{\mathrm{i}}) \right\rangle\!\!\right\rangle, \tag{1}$$

where the average over initial translational and rotational states of the target surface is denoted by $\langle\langle\ \rangle\rangle$, and the sum is over all unmeasured final states $\{n_{\mathrm{f}}\}$ of the surface which can scatter a projectile into its specified final state. The matrix elements of the transition operator $\hat{\mathcal{T}}$ are given by $\mathcal{T}_{\mathrm{fi}}$ and are taken with respect to unperturbed final and initial states of the system. The initial and final energies $\mathcal{E}_{\mathrm{i}}$ and $\mathcal{E}_{\mathrm{f}}$ refer to the total energy of the system of the projectile molecule plus the many-body surface target.

Taking the semiclassical limit, the transition rate is expressed as the Fourier transform of a generalized time-dependent correlation function. At this same level of approximation, it is assumed that the elastic part of the interaction potential commutes with the inelastic part, and the transition rate is then expressed as [44, 45]

$$w(\mathbf{p}_{\mathrm{f}}, \mathbf{l}_{\mathrm{f}}, \alpha_{l\mathrm{f}}; \mathbf{p}_{\mathrm{i}}, \mathbf{l}_{\mathrm{i}}, \alpha_{j\mathrm{i}}) = \frac{1}{\hbar^2} |\tau_{\mathrm{fi}}|^2 \int_{-\infty}^{\infty} \mathrm{e}^{-\mathrm{i}(E_{\mathrm{f}} - E_{\mathrm{i}})t/\hbar} \exp\{-2\mathcal{W}\} \exp\{\mathcal{Q}(t)\} \, \mathrm{d}t, \tag{2}$$

where $|\tau_{\mathrm{fi}}|^2$ is the scattering form factor, which in the decoupling approximation used in equation (2) is the square modulus of the off-energy-shell transition matrix of the elastic part of the interaction potential. The Debye–Waller factor $\exp\{-2\mathcal{W}\}$ includes contributions from translational, rotational and internal mode excitations and $\mathcal{Q}(t)$ is the generalized time-dependent correlation function. Within the decoupling approximation the Hamiltonian for each channel for energy transfers (i.e. surface elementary excitations, rotational excitations and internal vibrational modes) is considered independent and commutative with respect to the others. This results in the generalized correlation function $\exp\{\mathcal{Q}(t)\}$ being a product of independent correlation functions for each energy exchange channel, and the problem reduces to choosing models for the scattering kernels for each of these channels. However, each of these energy exchange mechanisms takes place while considering the energy gain or loss due to the other mechanisms. At this point it is interesting to make the connection to well-known models for atomic scattering; if phonons are the only mechanism for energy transfer then the approach of equation (2) leads to well-known transition rates that are Gaussian-like in both the translational energy transfer $E_{\mathrm{f}}^{\mathrm{T}} - E_{\mathrm{i}}^{\mathrm{T}}$ and the parallel component $\mathbf{P}$ of the momentum transfer $\mathbf{p} = \mathbf{p}_{\mathrm{f}} - \mathbf{p}_{\mathrm{i}}$ [46–49].

Including all three energy exchange channels in the generalized correlation function of equation (2), and taking the classical limits for translational and rotational motion, but retaining semiclassical quantum mechanics for the internal molecular vibrational modes, leads to the following general result for the state-to-state transition rate:

$$\begin{aligned} w(\mathbf{p}_{\mathrm{f}}, \mathbf{l}_{\mathrm{f}}; \mathbf{p}_{\mathrm{i}}, \mathbf{l}_{\mathrm{i}}) = {} & \frac{1}{\hbar^2} \, |\tau_{\mathrm{fi}}|^2 \left(\frac{2\pi\hbar^2 v_{\mathrm{R}}^2}{\Delta E_0 k_{\mathrm{B}} T_{\mathrm{S}}} \right) \left(\frac{2\pi\hbar^2 \omega_{\mathrm{R}}^2}{\Delta E_0^{\mathrm{R}} k_{\mathrm{B}} T_{\mathrm{S}}} \right)^{1/2} \\ & \times \left(\frac{\pi\hbar^2}{(\Delta E_0 + \Delta E_0^{\mathrm{R}}) k_{\mathrm{B}} T_{\mathrm{S}}} \right)^{1/2} \exp\left[-\frac{2\mathbf{P}^2 v_{\mathrm{R}}^2}{4\Delta E_0 k_{\mathrm{B}} T_{\mathrm{S}}} \right] \exp\left[-\frac{2 l_z^2 \omega_{\mathrm{R}}^2}{4\Delta E_0^{\mathrm{R}} k_{\mathrm{B}} T_{\mathrm{S}}} \right] \\ & \times \sum_{\kappa,\kappa'=1}^{N_{\mathrm{A}}} \left\{ \mathrm{e}^{\mathrm{i}(\mathbf{p}_{\mathrm{f}} \cdot \Delta\mathbf{r}_{\kappa,\kappa'}^{f} - \mathbf{p}_{\mathrm{i}} \cdot \Delta\mathbf{r}_{\kappa,\kappa'}^{i})/\hbar} \, \mathrm{e}^{-W_{\kappa}(\mathbf{p}_{\mathrm{f}}, \mathbf{p}_{\mathrm{i}})} \, \mathrm{e}^{-W_{\kappa'}(\mathbf{p}_{\mathrm{f}}, \mathbf{p}_{\mathrm{i}})} \right. \end{aligned}$$

$$\times \prod_{j=1}^{N_v} \sum_{\alpha_j=-\infty}^{\infty} I_{|\alpha_j|}(b_{\kappa,\kappa'}(\omega_j)) \left[\frac{n(\omega_j)+1}{n(\omega_j)}\right]^{\alpha_j/2}$$

$$\times \exp\left[-\frac{(E_{\rm f}^{\rm T}-E_{\rm i}^{\rm T}+E_{\rm f}^{\rm R}-E_{\rm i}^{\rm R}+\Delta E_0+\Delta E_0^{\rm R}+\hbar\sum_{s=1}^{N_v}\alpha_s\omega_s)^2}{4(\Delta E_0+\Delta E_0^{\rm R})k_{\rm B}T_{\rm S}}\right]\Bigg\}, \tag{3}$$

where $N_{\rm A}$ is the number of atoms in the projectile molecule, each denoted by index κ and mass m_κ, $E^{\rm T}$ and $E^{\rm R}$ are the respective translational and rotational energies of the molecule, $v_{\rm R}$ is a calculated average of phonon speeds parallel to the surface [46] and $\omega_{\rm R}$ is a similar constant for frustrated angular frequencies, $n(\omega_j)$ is the Bose–Einstein function for molecular vibrational frequency ω_j and $W_\kappa(\mathbf{p}_{\rm f},\mathbf{p}_{\rm i})$ is the Debye–Waller exponent associated with internal mode excitation. $I_{|\alpha_j|}(z)$ is the modified Bessel function of integer order α_j. The argument of the modified Bessel function of equation (3) is given by

$$b_{\kappa,\kappa'}(\omega_j)=\sum_{\beta,\beta'=1}^{3} p_\beta p_{\beta'}\frac{1}{N_v\hbar\sqrt{m_\kappa m_{\kappa'}}\omega_j}e(_j^\kappa|\beta)e^*(_j^{\kappa'}|\beta')\sqrt{n(\omega_j)[n(\omega_j)+1]}, \tag{4}$$

where $e(_j^\kappa|\beta)$ is the vibrational polarization vector for the jth internal mode and N_v is the total number of such modes.

The transition rate of equation (3) is expressed, for compactness, as a product over all normal modes labelled by j and a summation over the excitation quantum number denoted by α_j. To obtain the discrete state-to-state transition rate to a particular internal mode final state, or to a combination of states, one takes the corresponding (j,α_j)th term of equation (3). This general expression is readily expanded term by term in numbers of quanta excited for each of the internal modes, and often a consideration of only single quantum excitations is sufficient. The basic theory was initially applied to the case of acetylene scattering from the (001) surface of LiF [36, 50] in an attempt to explain state-to-state measurements taken by the group of Miller [1]. Their measurements for scattered angular distributions and final rotational temperatures were well explained by calculations based on equation (3) [50].

In many cases, such as where the incident molecular energy and the surface temperature are not large compared to the energy of internal molecular vibrational excitations, the expansion of equation (3) to only single quantum excitations is sufficient. This expansion is

$$w(\mathbf{p}_{\rm f},\mathbf{l}_{\rm f},\mathbf{p}_{\rm i},\mathbf{l}_{\rm i})=\frac{1}{\hbar^2}|\tau_{\rm fi}|^2\left(\frac{\pi\hbar^2}{(\Delta E_0+\Delta E_0^{\rm R})k_{\rm B}T_{\rm S}}\right)^{1/2}\left(\frac{2\pi\hbar^2v_{\rm R}^2}{\Delta E_0k_{\rm B}T_{\rm S}}\right)\left(\frac{2\pi\hbar^2\omega_{\rm R}^2}{\Delta E_0^{\rm R}k_{\rm B}T_{\rm S}}\right)^{1/2}$$

$$\times\exp\left[-\frac{2\mathbf{P}^2v_{\rm R}^2}{4\Delta E_0k_{\rm B}T_{\rm S}}\right]\exp\left[-\frac{2l_z^2\omega_{\rm R}^2}{4\Delta E_0^{\rm R}k_{\rm B}T_{\rm S}}\right]\sum_{\kappa,\kappa'=1}^{N_{\rm A}}{\rm e}^{{\rm i}(\mathbf{p}_{\rm f}\cdot\Delta\mathbf{r}_{\kappa,\kappa'}^f-\mathbf{p}_{\rm i}\cdot\Delta\mathbf{r}_{\kappa,\kappa'}^i)/\hbar}$$

$$\times{\rm e}^{-W_\kappa(\mathbf{p}_{\rm f},\mathbf{p}_{\rm i})}{\rm e}^{-W_{\kappa'}(\mathbf{p}_{\rm f},\mathbf{p}_{\rm i})}\Bigg\{\exp\left[-\frac{(E_{\rm f}^{\rm T}-E_{\rm i}^{\rm T}+E_{\rm f}^{\rm R}-E_{\rm i}^{\rm R}+\Delta E_0+\Delta E_0^{\rm R})^2}{4(\Delta E_0+\Delta E_0^{\rm R})k_{\rm B}T_{\rm S}}\right]$$

$$+\sum_{\gamma,\gamma'=1}^{3}p_\gamma p_{\gamma'}\sum_{j=1}^{N_v}\frac{1}{2\hbar N_v\sqrt{m_\kappa m_{\kappa'}}\omega_j}e(_j^\kappa|\gamma)e^*(_j^{\kappa'}|\gamma')$$

$$\times\Bigg(n(\omega_j)\exp\left[-\frac{(E_{\rm f}^{\rm T}-E_{\rm i}^{\rm T}+E_{\rm f}^{\rm R}-E_{\rm i}^{\rm R}+\Delta E_0+\Delta E_0^{\rm R}-\hbar\omega_j)^2}{4(\Delta E_0+\Delta E_0^{\rm R})k_{\rm B}T_{\rm S}}\right]$$

$$+(n(\omega_j)+1)\exp\left[-\frac{(E_{\rm f}^{\rm T}-E_{\rm i}^{\rm T}+E_{\rm f}^{\rm R}-E_{\rm i}^{\rm R}+\Delta E_0+\Delta E_0^{\rm R}+\hbar\omega_j)^2}{4(\Delta E_0+\Delta E_0^{\rm R})k_{\rm B}T_{\rm S}}\right]\Bigg)\Bigg\}. \tag{5}$$

Of the three terms in equation (5) the one proportional to $n(\omega_j)+1$ gives the single quantum creation rate, the term proportional to $n(\omega_j)$ is for single quantum annihilation, and the third term is the rate for scattering with no internal mode creation.

The experimental quantity usually measured in a surface scattering process is the differential reflection coefficient $\mathrm{d}^3R/\mathrm{d}\Omega_\mathrm{f}\,\mathrm{d}E_\mathrm{f}^\mathrm{T}$ giving the fraction of the incident particles which are scattered into a final solid angle of $\mathrm{d}\Omega_\mathrm{f}$ and energy interval $\mathrm{d}E_\mathrm{f}^\mathrm{T}$. This is obtained from the transition rate by dividing by the incident flux crossing a plane parallel to the surface and multiplying by the density of available final particle states

$$\frac{\mathrm{d}^3R}{\mathrm{d}\Omega_\mathrm{f}\,\mathrm{d}E_\mathrm{f}^\mathrm{T}}(\mathbf{p}_\mathrm{f},\mathbf{l}_\mathrm{f},\alpha_{lf},\mathbf{p}_\mathrm{i},\mathbf{l}_\mathrm{i},\alpha_{ji}) = \frac{L^4}{(2\pi\hbar)^3}\frac{m^2|\mathbf{p}_\mathrm{f}|}{p_{\mathrm{i}z}}\,w(\mathbf{p}_\mathrm{f},\mathbf{l}_\mathrm{f},\alpha_{lf},\mathbf{p}_\mathrm{i},\mathbf{l}_\mathrm{i},\alpha_{ji}). \tag{6}$$

Many experiments use a velocity dependent detector for which a correction must be applied. In the case of a density detector in which the detection probability is inversely proportional to the time of traversal, which is the case for the experiments of interest here, it should be divided by the final molecular translational speed. Also for the experiments considered here the incident molecular beam is in a mixture of rotational states corresponding approximately to an equilibrium distribution with a low temperature. Thus the differential reflection coefficient of equation (6) must be averaged over a Maxwell–Boltzmann distribution of incident energies as well as averaged over the molecular orientation and orientation of the angular momenta.

Equations (3) and (5) are appropriate to a smooth surface whose only corrugation is due to the thermal vibrations and rotations of its constituent molecules. The quantity v_R is a weighted average of phonon velocities parallel to the surface, whose value should be of the order or smaller than the Rayleigh mode speed [46]. Similarly, the quantity ω_R is a weighted average frequency for the parallel components of the frustrated rotational vibrations of the surface molecules [37]. The constant v_R is taken as a fitting parameter, just as has been done in all earlier work [46, 48]. In principle, v_R is well specified and can be calculated from basic principles, but this requires knowledge of the phonon spectral density at the position of the classical turning point of the potential energy. Knowledge of the spectral densities would also allow evaluation of the constant ω_R; however, thus far our calculations have used values of $\omega_\mathrm{R} < 10^{10}\ \mathrm{s}^{-1}$, sufficiently small that the results are independent of its choice.

The form factor $|\tau_\mathrm{fi}|^2$ appearing in equations (3) and (5) depends on the interaction potential. In many treatments of inelastic surface scattering the interaction potential is taken to be the repulsive part of the total molecule–surface interaction, which is approximately an exponentially decreasing function of the molecule–surface separation [51]. Thus the form factor amplitude τ_fi appropriate for use here is the transition matrix for the repulsive inelastic interaction. An expression which has been extremely useful, both for multiphonon scattering and for single phonon studies of atom–surface collisions [52, 53], is an expression given by the distorted wave Born approximation for an exponentially repulsive potential, first discussed by Jackson and Mott [54]. The Jackson–Mott matrix element, $\tau_\mathrm{fi} = v_\mathrm{JM}(p_{\mathrm{f}z}, p_{\mathrm{i}z})$, is the matrix element of an exponentially repulsive potential $V(z) = V_0\mathrm{e}^{-\beta z}$ taken with respect to its own eigenstates. Defining $q_\mathrm{i} = p_{\mathrm{i}z}/\hbar\beta$ and $q_\mathrm{f} = p_{\mathrm{f}z}/\hbar\beta$, it is given by

$$\tau_\mathrm{fi} = v_\mathrm{JM}(p_{\mathrm{f}z}, p_{\mathrm{i}z}) = \frac{\hbar^2\beta^2}{m}\frac{\pi q_\mathrm{i}q_\mathrm{f}(q_\mathrm{f}^2 - q_\mathrm{i}^2)}{\cosh(\pi q_\mathrm{f}) - \cosh(\pi q_\mathrm{i})}\left(\frac{\sinh(\pi q_\mathrm{f})\sinh(\pi q_\mathrm{i})}{q_\mathrm{i}q_\mathrm{f}}\right)^{1/2}. \tag{7}$$

In the semiclassical limit of a strongly repulsive surface barrier, which here corresponds to $\beta \to \infty$, the Jackson–Mott matrix element becomes [54, 55]

$$v_\mathrm{JM}(p_{\mathrm{f}z}, p_{\mathrm{i}z}) \to 2p_{\mathrm{f}z}p_{\mathrm{i}z}/m. \tag{8}$$

The same expression as equation (8) is obtained for other potentials in the limit of a strongly repulsive surface barrier, including the Morse potential and a simple Heaviside step potential.

For this work, equation (8) was used as the form factor, after modification by the addition of an attractive well. For classical translational motion, such as considered here, the major effects of the adsorption well in the potential are to accelerate the incoming projectiles and to

refract them into directions more normal to the surface plane. The acceleration and refraction are independent of the shape of the attractive part of the well, so we have used the simplest approximation, that of a square well. Upon entering the attractive well the energies are transformed according to $E'^{\mathrm{T}}_q = E^{\mathrm{T}}_q + |D|$, where D is the well depth, but all of this increased energy is associated with the perpendicular motion, hence

$$p'^2_{qz} = p^2_{qz} + 2m|D|. \tag{9}$$

The differential reflection coefficient of equation (6) is then modified by multiplying by the Jacobian determinant relating energy and solid angle inside and outside of the well.

The final quantities to be specified are the polarization vectors $e(^{\kappa}_{j}|\gamma)$ for the internal vibrational modes of the molecule. For the case of the diatomic molecular projectile O_2 there is only one normal mode and its polarization vector is unity. For the case of CH_4 the polarization vectors were calculated using a standard classical normal modes analysis in the harmonic approximation [56–58]; there are a total of nine normal modes that have four different frequencies called ν_1, ν_2, ν_3 and ν_4 at the energies of 361.7, 190.2, 374.3 and 161.9 meV, respectively [57]. The ν_1 and ν_3 modes are singly and triply degenerate stretching modes at higher frequencies that are not expected to be appreciably excited at low collision energies. The double and triply degenerate bending modes ν_2 and ν_4 at lower energies are of interest in the present study because they are the ones that will be excited for incident translational energies of up to 0.5 eV. The parameters involved in this normal modes calculation are the length of the C–H bond, which is $l_{\mathrm{CH}} = 1.0862$ Å [59]; the H–C–H equilibrium angle of $109°28'$, and five force constants [59–61] with the following values: two stretching force constants $F_{11} = 5.435$ aJ Å^{-2} and $F_{33} = 5.378$ aJ Å^{-2} where a $= 10^{-18}$, two angle bending force constants $F_{22} = 0.584$ aJ rad^{-2} and $F_{44} = 0.548$ aJ rad^{-2}, and one mixed constant $F_{43} = -0.221$ aJ Å^{-1} rad^{-1}.

3. Results

3.1. Methane scattering from LiF(001)

The experimental measurements discussed here for scattering of CH_4 from a clean ordered LiF(001) surface were carried out with an incident molecular beam whose translational energy varied between 190 and 500 meV by heating the supersonic jet nozzle and seeding with helium gas [15]. Surface temperatures were varied from 300 to 700 K. The impinging molecules were reflected from the LiF(001) surface, and all measurements were carried out in the scattering plane, which contains the incident beam and the surface normal. With the detector positioned at a fixed angle of 90° from the incident beam, the incident and final angles at which all measurements were taken are related by $\theta_{\mathrm{f}} = 90° - \theta_{\mathrm{i}}$.

An example of TOF energy-resolved spectra compared with calculations based on equation (5) is shown in figure 1. The experimental data are exhibited as points for three incident energies: 500, 350 and 190 meV as marked, and for $\theta_{\mathrm{i}} = 30°$. The surface temperature is 300 K and the crystal azimuthal direction is ⟨110⟩. The vertical lines indicate the TOF time for elastic scattering (dashed line) and the time corresponding to recoil energy loss for hard sphere scattering at these angles (dashed–dotted line).

The calculations from equation (5) are shown as solid curves in figure 1. These calculations are the sum of the differential reflection coefficient over all final rotational angular momenta and all molecular internal modes, and are for a potential well depth of zero, a rotational temperature of the incident beam of 30 K, and an incident beam vibrational temperature of 10 K. The rotational temperature of the incident beam is estimated to be about 30–40 K, while

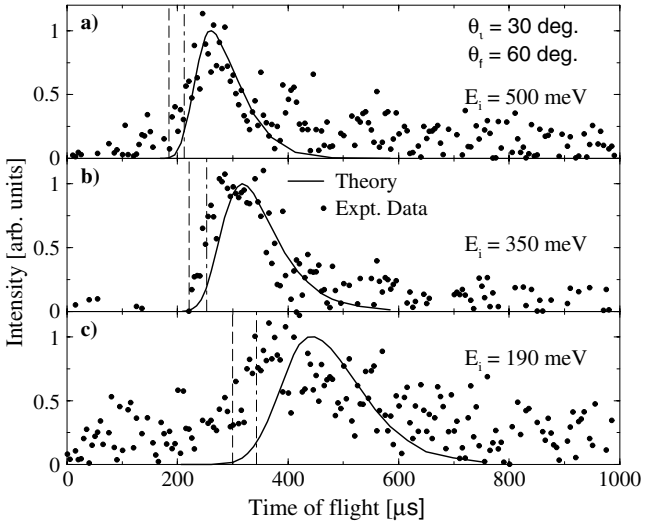

Figure 1. Time of flight distributions of CH_4 molecules scattered from a LiF(001) surface in the ⟨110⟩ azimuthal direction for three different translational energies: 500 meV (a); 350 meV (b); 190 meV (c). The incident angle is $\theta_i = 30°$ and the surface temperature is 300 K. The experimental measurements are shown as data points and the calculations are shown as solid curves. Two vertical lines indicate recoil energy loss (dashed–dotted line) and elastic scattering (dashed line).

the experimental vibrational temperature is estimated to be near room temperature [15]. The calculated results are insensitive to either of these parameters within these ranges. The principal moments of inertia of the CH_4 and LiF molecules were calculated classically with the known atomic masses and molecular bonding distances, leading to values of the principal moments of inertia of $I_M = 5.26 \times 10^{-47}$ kg m^2 for CH_4 and $I_C = 3.41 \times 10^{-46}$ kg m^2 for LiF. As explained above in section 2 the velocity v_R was taken as a parameter, since a realistic evaluation requires knowledge of the complete phonon spectral density at the classical turning point. v_R is expected to be of the order or smaller than the Rayleigh speed, which is approximately 4000 m s^{-1} for LiF(001) [62]. For the calculations on the CH_4/LiF(001) system the value $v_R = 1500$ m s^{-1} was used as this provides a reasonable fit to all data for both TOF spectra and angular distributions. Interestingly, decreasing v_R by a factor of two has very little effect on the position of the maximum in the calculated TOF distribution, but it increases the width by about 10%, particularly on the large time side. Conversely, increasing v_R by a factor of two narrows the distribution by about 10% but again leaves the maximum in nearly the same position. For the value of M_C, the effective mass of the surface molecules, we have used three times the mass of a LiF molecule. A larger effective mass indicates a collective effect in which the incident projectile is colliding with more than a single LiF molecule. The initial analysis using the washboard model carried out by Yamamoto *et al* also required surface masses several times larger than that of a single LiF [15]. The good agreement between calculations and experiment seen in figure 1 holds over the entire range of incident angles measured, from $\theta_i = 30°$ to 50°.

Figure 2 shows experimental data for angular intensity distributions for methane scattered from LiF(001) ⟨110⟩ together with the calculated curves represented by solid curves. The surface temperature is 300 K. Three different incident energies are shown in figure 2, $E_i^T = 190$, 350 and 500 meV as marked. At the smallest incident energy the angular distributions are broad and the angular position of the most probable intensity is somewhat

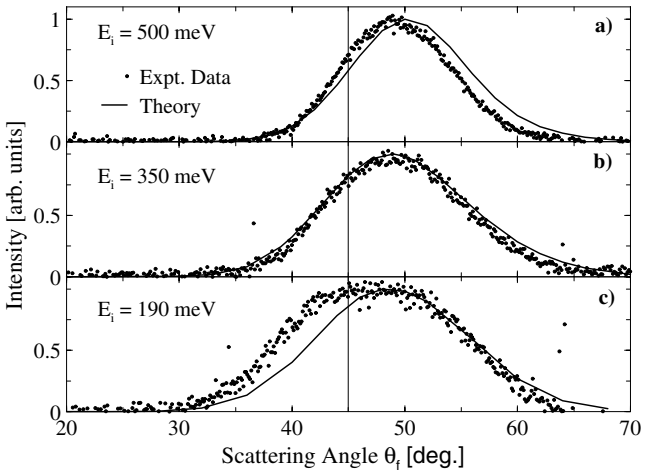

Figure 2. Angular intensity distributions for methane CH_4 scattered from a LiF(001) surface in the ⟨110⟩ azimuthal direction together with the calculated curves. The incident translational energies are: (a) 500 meV; (b) 350 meV; (c) 190 meV. The surface temperature is 300 K. The solid curves are the calculations. The vertical line marks the specular position.

larger than the specular position of 45° denoted by the solid vertical line. With increasing incident energy the width of the angular distribution narrows and the most probable final angle increases, and at all energies the theoretical curves give a reasonable explanation of the data. This decrease with energy of the full width at half maximum (FWHM) and concomitant supraspecular shift of the most probable final angle is very similar to the behaviour previously observed in the typical fixed incident angle distributions for rare gas scattering [63] and molecular scattering [1, 35].

Measurements of the angular distributions were made over a range of surface temperatures from 200 to 700 K. As a function of temperature the most probable scattering angle of the angular distribution decreases slowly (subspecular shift), and the full width at half maximum of the distribution shows a monotonic increase. Both of these effects were well explained by the calculations.

Measurements of rotational excitation were not made in the experiments of Yamamoto *et al*, however, figure 3 shows a prediction of the calculated scattered intensity as a function of rotational energy E_f^R for incident angle $\theta_i = 41°$ and for incident translational energies 75, 190, 350 and 500 meV, respectively. The quantity calculated is the differential reflection coefficient of equation (6) averaged over an initial Maxwell–Boltzmann distribution of rotational states with a temperature $T_R = 30$ K, and summed over final translational energies and all internal vibrational mode excitations. All parameters are the same as were used in the calculations for figure 2. For the three highest incident energies the intensity falls off rapidly as a function of E_f^R for the first 15 meV, and then takes on nearly exponentially decreasing behaviour as indicated by the curves becoming nearly straight lines in this logarithmic graph. For the nearly straight-line region for $E_f^R > 30$ meV we can extract an effective final rotational temperature for each incident energy through comparison with a Maxwell–Boltzmann distribution. The final effective rotational temperature increases with increasing incident energy and the values are 359, 595 and 838 K for $E_i^T = 190$, 350 and 500 meV, respectively.

These final rotational temperatures are consistent with the range measured for the scattering of C_2H_2 from LiF(001) by Miller *et al* [1]. That group also made an independent measure of

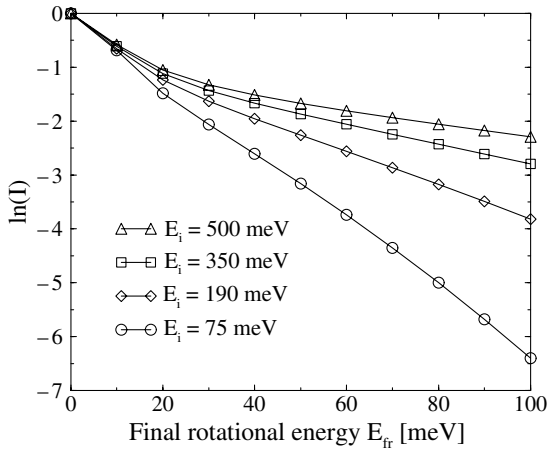

Figure 3. Scattered intensity versus final rotational energy for CH_4 scattering from a LiF(001) surface at room temperature. The incident translational energy is $E_i = 75$, 190, 350 and 500 meV as marked.

the effective final rotational temperature for CH_4 /LiF(001) at a lower incident translational energy of 75 meV [64]. This measurement gave the rotational temperature of scattered methane molecules of 240 K. Our calculations at 75 meV show nearly exponential behaviour at all final rotational energies and give a final rotational temperature of 212 K, in reasonable agreement.

3.2. Oxygen scattering from Al(111)

Figure 4 shows comparisons of angular distribution data [35] with theory for the O_2/Al(111) system. The solid curves are calculations for a potential with well depth $D = 50$ meV and the dash–dotted curves are for $D = 0$. The calculations are averaged over an incident beam with a Maxwell–Boltzmann distribution of rotational energies with rotational temperature 35 K, and the parameter $v_R = 2300$ m s^{-1}. Direct measurement of the rotational state of the O_2 incident beam was not possible in the experiment, but an indirect measure was provided by substituting NO gas under the same experimental conditions. An unseeded, room-temperature NO beam had a rotational temperature of 36 K, and it is expected that the rotational temperature of O_2 under the same conditions will be comparable. However, as with the case of CH_4 the calculations are insensitive to such small incident rotational temperature values. It is seen that the theory predicts broad angular distributions with FWHMs of about 20° and peak maxima located near the specular positions or slightly supraspecular, in reasonable agreement with experiment. The anomalous sticking behaviour observed with this system has been associated with a weak physisorption well that varies in depth depending on surface position, with its deepest point of about 100 meV at the same site in the surface unit cell as the maximum in the barrier towards dissociative adsorption [39]. In the present calculations, a simpler uniform square-well model of depth roughly the average of the previous work [39] is used in order to test the effects of a physisorption well on the scattering behaviour. Including a well in the interaction shifts the calculated angular distribution slightly in the supraspecular direction and broadens the peaks. This shift can be understood on the basis of the larger average energy losses caused by the molecule colliding with the repulsive surface at a higher effective energy and a more normal collision angle inside the well. Overall, the calculations with a 50 meV well seem to agree somewhat better with the experiment than those without a well.

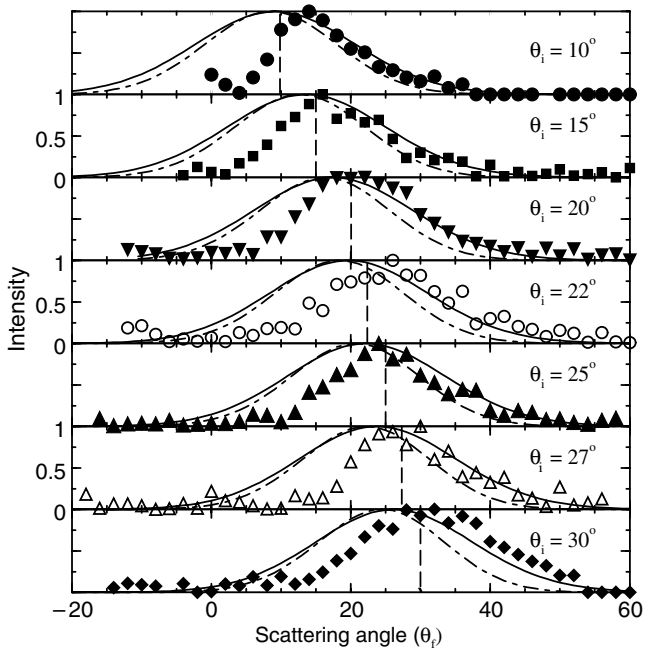

Figure 4. Angular distributions of the O_2/Al(111) scattering intensity for different incident angles as shown with an incident energy $E_i = 90$ meV and surface temperature $T_S = 298$ K. The experimental data points are shown as symbols. The calculated results are shown as solid curves for a potential with well depth $D = 50$ meV, and as dash–dotted curves for $D = 0$. The vertical dashed line marks the specular position.

It is noticeable that for the smaller incidence angles in figure 4 the experimental points appear to lie below the calculated curves at final angles near normal. This disagreement may be an artifact of correcting the scattered intensity for the small fraction of the incident beam that can enter the detector when the detector and incident beam directions are close to each other. The design of the detector consists of a tube open at both ends, so it will count O_2 molecules that enter from either direction. When the detector is brought near to the incident beam direction, which is the case for the scattering angles near the surface normal measured for incident beam angles also near normal, a small number of O_2 molecules in the tail of the angular spread enter the detector from the back end and are counted before striking the surface. A correction for this has been made, but in the case of incident angles smaller than 20° an over-compensation of the correction may account for the apparent discrepancy between experiment and theory.

Measurements were also made for angular distributions at fixed incident angle as a function of surface temperature. The most noticeable effect was a subspecular shift of the peak intensity with increasing surface temperature. This subspecular shift was well described by the calculations [65], and the physical explanation of this shift is discussed in the paragraphs below.

Near specular and certainly subspecular angular distribution lobes, such as seen in figure 4, are not expected on the basis of predictions from simple theoretical models that do not allow for parallel momentum exchange with the surface. In situations such as this where the mass ratio of the projectile molecule to that of the surface atoms is large, and where the incident energy is large compared to the temperature of the surface, the typical molecule will lose a large fraction of its energy. In fact, energy-resolved calculations show that under the present

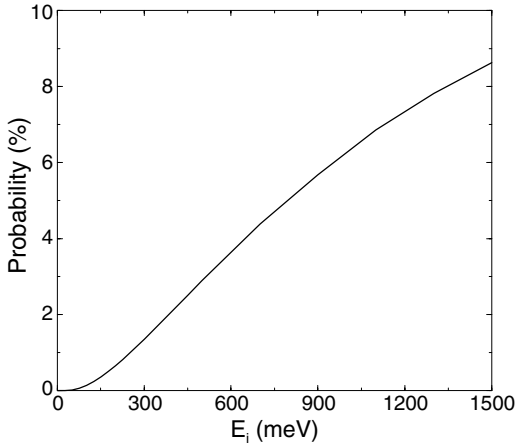

Figure 5. The calculated excitation probability of the O_2 internal stretch mode as a function of incident translational energy; $\theta_i = 15°$, $\theta_f = 45°$ and the surface temperature is $T_S = 300\ K$.

conditions the O_2 may lose substantially more than half its incident energy upon collision. Thus, if the parallel momentum of the projectile is not allowed to change, the perpendicular momentum will become much smaller, which would predict a distinctly supraspecular angular distribution lobe.

However, the theoretical models of equations (3) and (5) allow for the correct transfer of momentum parallel to the surface, i.e. the parallel momentum of the scattered particle is equal to the parallel momentum of the incident particle plus whatever parallel momentum is gained or lost to the phonons exchanged. Perpendicular momentum, on the other hand, is not conserved due to the broken symmetry presented by the surface. Perpendicular momentum is indeed exchanged with the surface, but there is no conservation law in that direction. Thus, the projectile's final perpendicular momentum is determined by the combined laws of energy conservation and parallel momentum conservation. The behaviour of the angular distribution with increasing temperature is explained by the fact that, at higher temperatures, the incoming projectiles lose less energy on average. Thus, perpendicular momentum loss is decreased relative to the exchange of parallel momentum, resulting in a subspecular shift.

It is of interest to show predictions of the full molecular scattering theory of equation (3) for the excitation probability of the molecular internal vibrational mode. At the incident energies involved in the present experiments, the O–O stretch mode, which in the gas phase has a value of 193 meV, is not appreciably excited. However, shown in figure 5 is a calculation of the excitation probability for the first excited state of this mode as a function of incident translational energy. As for the previous calculations, a rotational temperature of 35 K is assumed for the incident beam, and the incident and final angles are $\theta_i = 15°$ and $\theta_f = 45°$. No correction has been made for the fact that the dissociative sticking becomes large at energies approaching 1 eV. It is seen that the internal mode excitation probability does not become appreciable until well above the mode excitation energy, after which it increases, reaches a maximum and then eventually decreases, as expected. However, it is interesting to note that due to energy supplied by the surface phonons there is a small but non-zero probability of excitation even for incident translational plus rotational energy less than the excitation energy, in the range where the observed sticking is still small compared to unity. This is clearly observed in figure 5 where the excitation probability is small but non-zero for incident energies substantially less than the 190 meV threshold.

Such behaviour is reminiscent of recent observations of phonon energy coupling to the rotational motion as was recently reported by the group of Sitz (University of Texas, Austin) for the case of molecular hydrogen and deuterium reflected from metal surfaces [2]. They observed scattered molecules leaving the surface in rotational states having energy greater than the incident translational energy, which is possible only if thermal energy from the surface is transferred to the rotations, and such energy transfers have been supported by recent calculations [66, 67].

Our theory, even at its present level, contains mechanisms for coupling energy transfer between the various degrees of freedom, as is clearly seen in calculations of the probability of excitation of internal vibrational modes. Internal mode excitation probabilities are calculated to be non-zero at incident translational energies smaller than the $h\nu$ required to create a single quantum due to conversion of rotational energy and energy from the phonons of the surface into vibrational energy [65, 68].

4. Conclusions

This paper presents a theoretical analysis of recently available data for the scattering of CH_4 from a clean, ordered LiF(001) surface and O_2 scattering from Al(111). The theory used is one that treats the translational and rotational motion of the projectile molecules with classical mechanics while using a semiclassical treatment for the excitation of internal molecular vibrational modes [36]. The origins of this theory lie in classical treatments that have been successful in describing atom–surface scattering under conditions in which the numbers of exchanged phonons is large [46, 48, 63]. The molecular scattering theory was first applied to the case of scattering of C_2H_2 from a LiF surface [37] where it gave a reasonable description of the observed measurements [64] for angular distributions and rotational energy excitation. The present work shows that for two additional systems the theory is capable of describing the basic dependence of the observed angular distributions and translational energy-resolved spectra as functions of the experimentally controllable parameters, i.e. the incident angle, beam energy and surface temperature.

In addition to carrying out calculations for comparison with available data, results of a more predictive nature are shown giving probabilities for excitation of the internal degrees of freedom of the molecular projectile. These indicate that measurements of the intensity as a function of final rotational energy, or measurements of molecular vibrational excitation, can provide important physical information on the coupling of translational, vibrational and rotational motion during the collision process.

In general, the theoretical model used to analyse these scattering experiments demonstrates how far one can go towards obtaining quantitative agreement with available data for scattering of small molecules from the LiF(001) surface without introducing a great amount of detail into the scattering potential. The dependence of the measured angular distributions and energy resolved spectra on incident angle, surface temperature and incident translational energy appear to be largely governed by the mechanism of transfers of large numbers of phonons, and this mechanism is well treated by the present formalism.

An overall conclusion of this work is that the physical mechanism causing the shapes and behaviours of the measured angular distributions is largely dominated by energy exchange with the phonon distribution of the surface. Rotational energy exchange in the collision process has a noticeable effect, but is much less influential than the conversion of translational energy to surface vibrational energy. The energy-resolved calculations show that for translational energies large compared to the surface temperature, on average energy is lost when the molecule strikes the surface and that the typical energy loss can be large compared to the incident energy.

Such large losses of translational energy to the phonon field, as observed in that fraction of incoming atoms that are scattered, will surely also have a strong effect on chemisorption which is an important interaction channel for these systems. The present approach demonstrates that the exchange of phonon energy with the surface can be handled in a straightforward theoretical manner.

Acknowledgments

This work was supported by the National Science Foundation under grant number DMR-0089503 and by the Department of Energy under grant number DE-FG02-98ER45704. The authors would like to thank S Yamamoto, T Kondo, E Hasselbrink and O Weiße for helpful discussions during the course of this work.

References

[1] Francisco T W, Camillone N III and Miller R E 1996 *Phys. Rev. Lett.* **77** 1402
[2] Watts E and Sitz G O 1999 *J. Chem. Phys.* **111** 9791
[3] Behr P, Morris J R, Antman M D, Ringeisen B R, Splan J R and Nathanson G M 2001 *Geophys. Res. Lett.* **28** 1961
[4] Kondo T, Tomii T, Hiraoka T, Ikeuchi T, Yagyu S and Yamamoto S 2000 *J. Chem. Phys.* **112** 9940
[5] Berenbak B, Zboray S, Papageorgopoulos D C, Stolte S and Kleyn A W 2002 *Phys. Chem. Chem. Phys.* **4** 68
[6] Mortensen H, Jensen E, Diekhöner L, Baurichter A, Luntz A C and Petrunin V V 2003 *J. Chem. Phys.* **118** 11200
[7] Kleyn A W, Luntz A C and Auerbach D J 1981 *Phys. Rev. Lett.* **47** 1169
[8] Mödl A, Robota H, Segner J, Vielhaber W, Lin M C and Ertl G 1985 *J. Chem. Phys.* **83** 4800
[9] Andersson T, Althoff F, Linde P, Hassel M, Persson M and Andersson S 2000 *J. Chem. Phys.* **113** 9262
[10] Maazouz M, Barstis T L O, Maazouz P L and Jacobs D C 2000 *Phys. Rev. Lett.* **84** 1331
[11] Libuda J, Meusel I, Hartmann J and Freund H-J 2000 *Rev. Sci. Instrum.* **71** 4395
[12] Huang Y, Wodtke A M, Hou H, Rettner C T and Auerbach D J 2000 *Phys. Rev. Lett.* **84** 2985
[13] Wodtke A M, Huang Y and Auerbach D J 2003 *J. Chem. Phys.* **118** 8033
[14] Shuler S F, Davis G M and Morris J R 2002 *J. Chem. Phys.* **116** 9147
[15] Tomii T, Kondo T, Hiraoka T, Ikeuchi T, Yagyu S and Yamamoto S 2000 *J. Chem. Phys.* **112** 9052
[16] Yagu S, Hiraoka T, Kino Y and Yamamoto S 2000 *Appl. Surf. Sci.* **165** 217
[17] Kondo T, Tomii T, Yagu S and Yamamoto S 2001 *J. Vac. Sci. Technol.* A **19** 2468
[18] Kondo T, Sasaki T and Yamamoto S 2002 *J. Chem. Phys.* **116** 7673
[19] Hou H, Huang Y, Gulding S J, Rettner C T, Auerbach D J and Wodtke A M 1999 *J. Chem. Phys.* **110** 10660
[20] Michelsen H A, Rettner C T and Auerbach D J 1992 *Surf. Sci.* **272** 65
[21] Rettner C T, Auerbach D J and Michelsen H A 1992 *Phys. Rev. Lett.* **68** 1164
[22] Rettner C T, Kimman J and Auerbach D J 1991 *J. Chem. Phys.* **94** 734
[23] Maazouz M, Maazouz P L and Jacobs D C 2002 *J. Chem. Phys.* **117** 10917
[24] Morris J R, Kim G, Barstis T L O, Mitra R and Jacobs D C 1997 *J. Chem. Phys.* **107** 6448
[25] McCabe P R, Juurlink L B F and Utz A L 2000 *Rev. Sci. Instrum.* **71** 42
[26] Ohashi M and Ozeki M 2001 *Appl. Phys. Lett.* **79** 500
[27] Ainsworth M K, McCombie J, McCoustra M R S and Chesters M A 2000 *J. Chem. Phys.* **113** 8762
[28] Gleeson M A, Kropholler M and Kleyn A W 2000 *Appl. Phys. Lett.* **77** 1096
[29] Watts E and Sitz G O 2001 *J. Chem. Phys.* **114** 4171
[30] Watts E, Sitz G O, McCormack D A, Kroes G J, Olsen R A, Groeneveld J A, Van Stralen J N P, Baerends E J and Mowrey R C 2001 *J. Chem. Phys.* **114** 495
[31] Gostein M and Sitz G O 1997 *J. Chem. Phys.* **106** 7378
[32] Janda K C, Hurst J E, Cowin J, Wharton L and Auerbach D J 1983 *Surf. Sci.* **130** 395
[33] Luntz A C and Bethune D S 1989 *J. Chem. Phys.* **90** 1274
[34] Schoofs G R, Arumainayagam C R, McMaster M C and Madix R J 1989 *Surf. Sci.* **215** 1
[35] Weiße O, Wesenberg C, Binetti M and Hasselbrink E 2003 *J. Chem. Phys.* **118** 8010
[36] Iftimia I and Manson J R 2001 *Phys. Rev. Lett.* **87** 93201
[37] Iftimia I and Manson J R 2002 *Phys. Rev.* B **65** 125401

[38] Österlund L, Zorić I and Kasemo B 1997 Dissociative sticking of O_2 on Al(111) *Phys. Rev.* B **55** 15452
[39] Weiße O, Wesenberg C, Binetti M, Hasselbrink E, Corriol C, Darling G R and Holloway S 2003 *J. Chem. Phys.* **118** 8010
[40] Kondo T, Sasaki T and Yamamoto S 2002 *J. Chem. Phys.* **116** 7673
[41] Yagu S, Kino Y, Ozeki K and Yamamoto S 1999 *Surf. Sci.* **433–435** 779
[42] Logan R M and Stickney R E 1966 *J. Chem. Phys.* **44** 195
[43] Tully J C 1990 *J. Chem. Phys.* **92** 680
[44] Bortolani V and Levi A C 1986 *Riv. Nuovo Cimento* **9** 1
[45] Celli V, Himes D, Bortolani V, Santoro G, Toennies J P and Zhang G 1991 *Surf. Sci.* **242** 518
[46] Brako R and Newns D M 1982 *Phys. Rev. Lett.* **48** 1859
[47] Brako R and Newns D M 1982 *Surf. Sci.* **123** 439
[48] Meyer H-D and Levine R D 1984 *Chem. Phys.* **85** 189
[49] Manson J R 1994 *Comput. Phys. Commun.* **80** 145
[50] Iftimia I and Manson J R 2002 *Phys. Rev.* B **65** 125412
[51] Hulpke E (ed) 1992 *Helium Atom Scattering from Surfaces* (*Springer Series in Surface Science*) (Berlin: Springer)
[52] Celli V, Himes D, Tran P, Toennies J P, Wöll Ch and Zhang G 1991 *Phys. Rev. Lett.* **66** 3160
[53] Hofmann F, Toennies J P and Manson J R 1994 *J. Chem. Phys.* **101** 10155
Hofmann F, Toennies J P and Manson J R 1997 *J. Chem. Phys.* **106** 1234
[54] Jackson J M and Mott N F 1932 *Proc. R. Soc.* A **137** 703
[55] Goodman F O and Wachman H Y 1976 *Dynamics of Gas–Surface Scattering* (New York: Academic)
[56] Wilson E B, Decius J C and Cross P C 1955 *Molecular Vibrations. The Theory of Infrared and Raman Vibrational Spectra* (New York: McGraw-Hill)
[57] Nakamoto K 1970 *Infrared Spectra of Inorganic and Coordination Compounds* (New York: Wiley)
[58] Woodward L A 1972 *Introduction to the Theory of Molecular Vibrations and Vibrational Spectroscopy* (Oxford: Oxford University Press)
[59] Lee T J, Martin J M L and Taylor P R 1995 *J. Chem. Phys.* **102** 254
[60] Gray D L and Robiette A G 1979 *Mol. Phys.* **37** 1901
[61] Raynes W T, Lazzeretti P, Zanasi R, Sadlej A J and Fowler P W 1987 *Mol. Phys.* **60** 509
[62] Kaye G W C and Laby T H 1986 *Tables of Physical and Chemical Constants and Some Mathematical Functions* (London: Longman)
[63] Muis A and Manson J R 1999 *J. Chem. Phys.* **111** 730
[64] Wight A C and Miller R E 1998 *J. Chem. Phys.* **109** 1976
[65] Ambaye H, Manson J R, Weiße O, Wesenberg C, Binetti M and Hasselbrink E 2004 *J. Chem. Phys.* at press
[66] Wang Z S, Darling G R and Holloway S 2001 *Phys. Rev. Lett.* **87** 226102
[67] Busnengo H F, Dong W, Sautet P and Salin A 2001 *Phys. Rev. Lett.* **87** 127601
[68] Moroz I and Manson J R 2004 *Phys. Rev.* B at press